

## Controlled Growth of 2D/2D Heterojunction for High- Performance Sodium Ion Storage

Shujin Cheng <sup>a,b</sup>, Zicheng Zuo <sup>\*a</sup>, Yuliang Li <sup>\*a,b</sup>

a. Beijing National Laboratory for Molecular Sciences (BNLMS), CAS Research/Education Center for Excellence in Molecular Sciences, Institute of Chemistry, Chinese Academy of Sciences, Beijing 100190, P. R. China

b. Department of Chemistry, University of Chinese Academy of Sciences, Beijing 100049, P. R. China

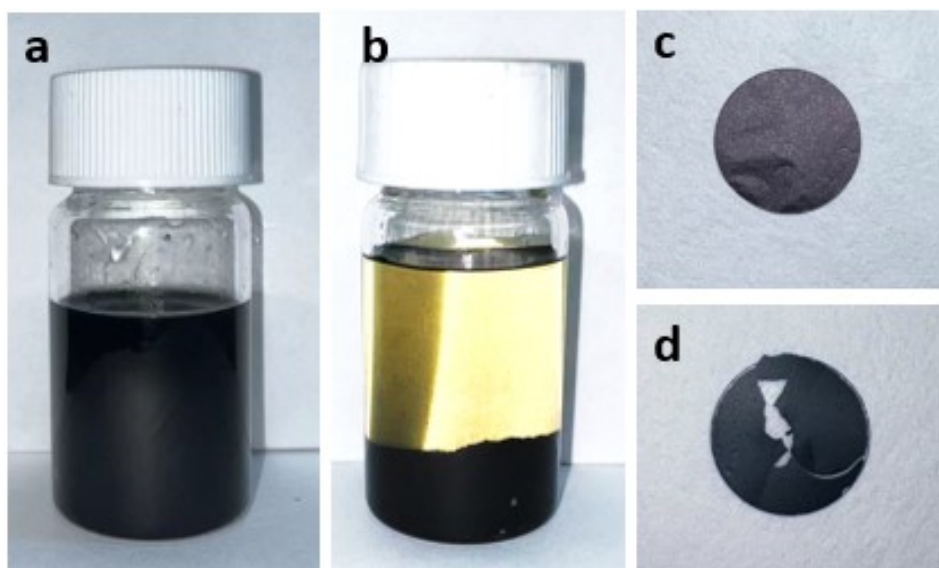


Figure S1. Photo of  $Ti_3C_2T_x$  before and after GDY modification. a)  $Ti_3C_2T_x$  solution before GDY modification, b)  $Ti_3C_2T_x$  solution after GDY modification, c) binder-free electrode of  $Ti_3C_2T_x$ , d) binder-free electrode of  $Ti_3C_2T_x@GDY$ .

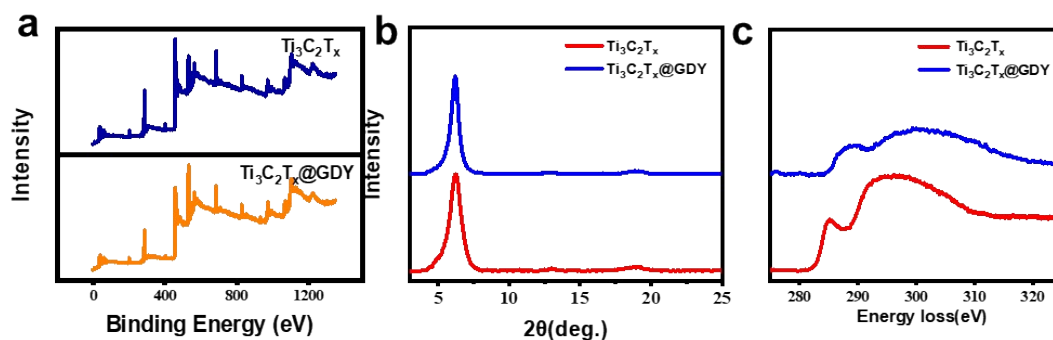


Figure S2. a) XPS spectra of  $Ti_3C_2T_x$  and  $Ti_3C_2T_x@GDY$ , b) XRD patterns of  $Ti_3C_2T_x$  and  $Ti_3C_2T_x@GDY$ , c) the energy loss spectra of C element.

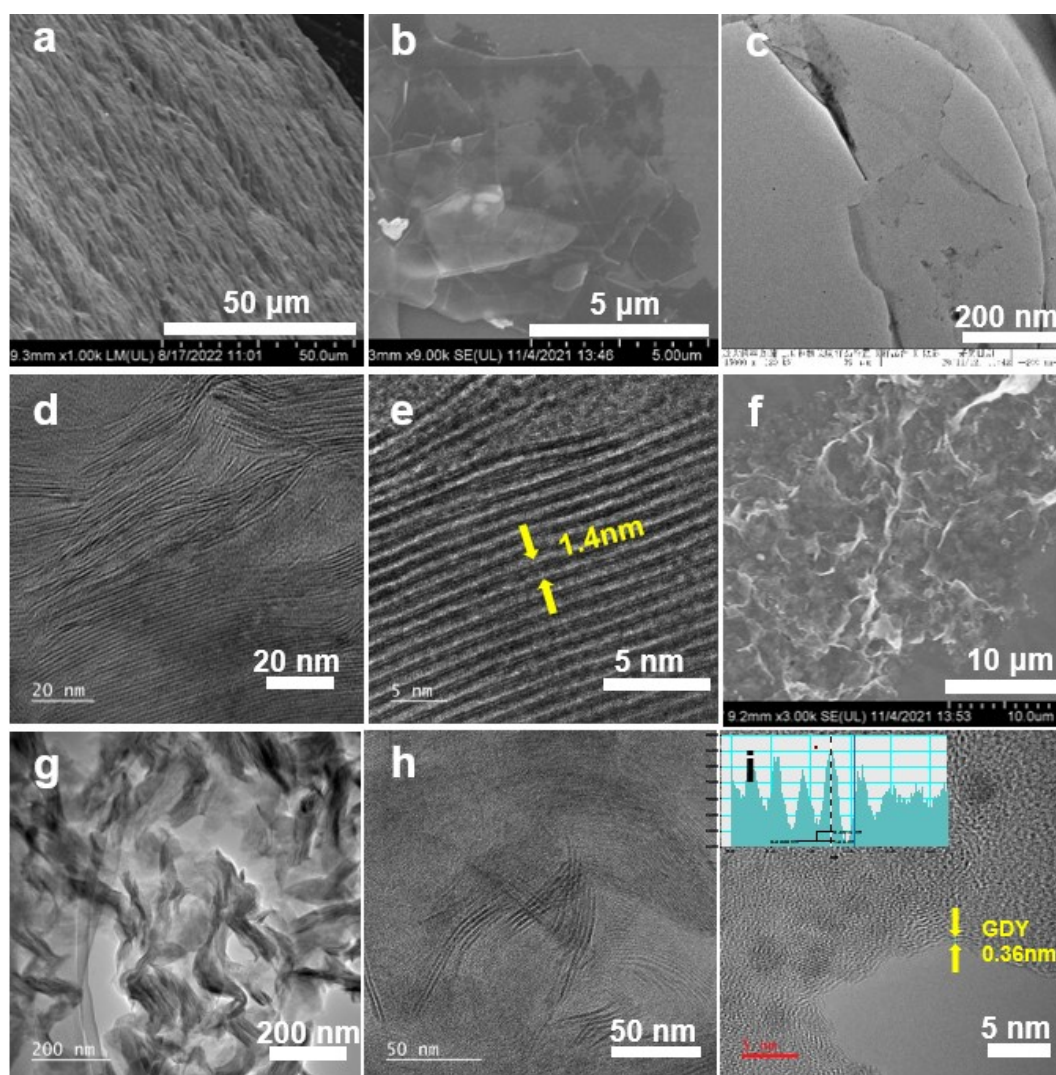


Figure S3. a)-b) SEM and c)-e) TEM images of the pristine  $Ti_3C_2T_x$  nanosheets; f) SEM and g)-i) TEM image of  $Ti_3C_2T_x@GDY$ , inset in i is the interlayer distance of GDY.

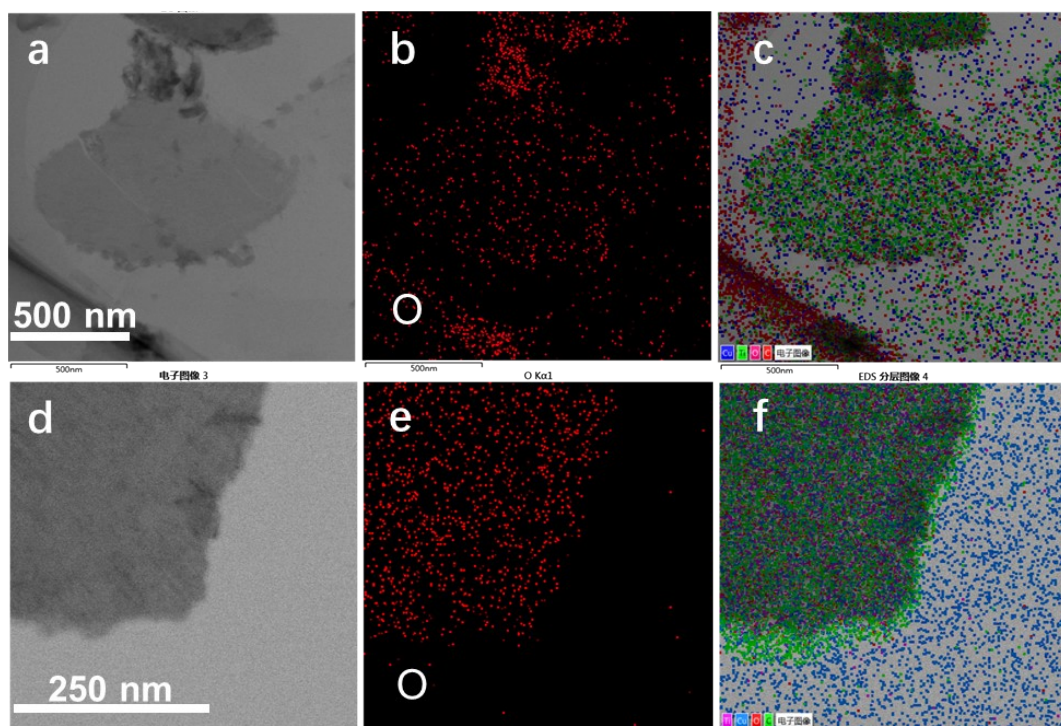


Figure S4. a)-c) the C elemental distribution and superposition of elements of bare  $\text{Ti}_3\text{C}_2\text{T}_x$ , d)-f) the elemental distribution images of  $\text{Ti}_3\text{C}_2\text{T}_x$ @GDY and superposition of elements of bare  $\text{Ti}_3\text{C}_2\text{T}_x$ .

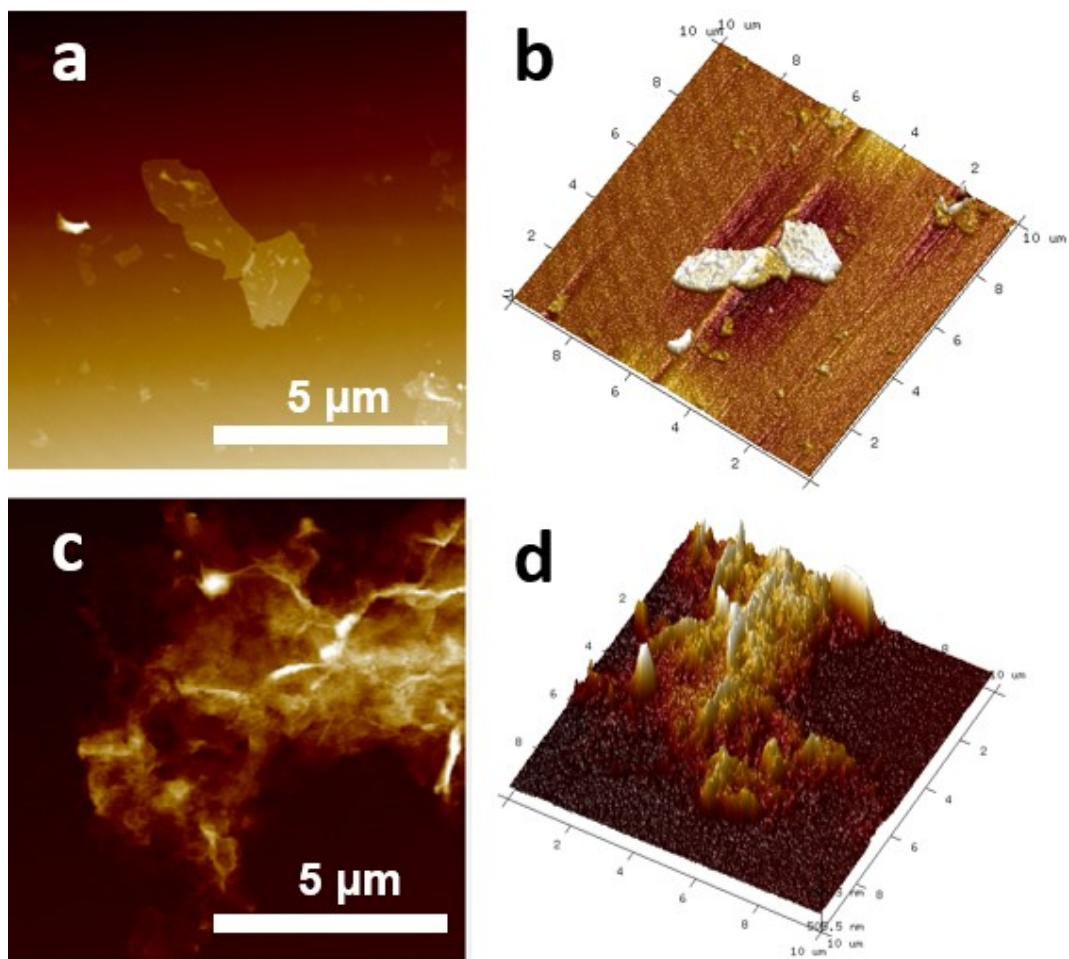


Figure S5. a) 2D and b) 3D AFM images of the  $\text{Ti}_3\text{C}_2\text{T}_x$ ; c) 2D and d) 3D AFM images of the  $\text{Ti}_3\text{C}_2\text{T}_x@\text{GDY}$ .

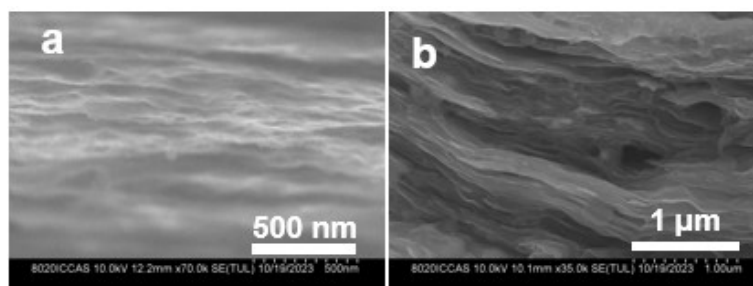


Figure S6. SEM images of the structure after the long-term cycling in a)  $\text{Ti}_3\text{C}_2\text{T}_x$  and b)  $\text{Ti}_3\text{C}_2\text{T}_x@\text{GDY}$ .



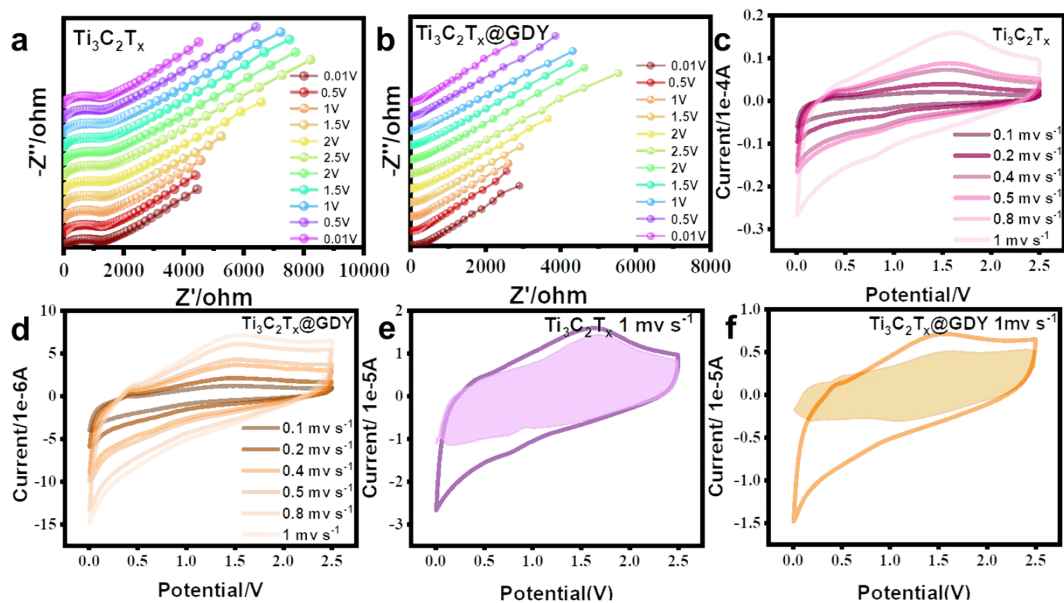


Figure S7. Electrochemical impedance spectroscopy of a)  $\text{Ti}_3\text{C}_2\text{T}_x$  and b)  $\text{Ti}_3\text{C}_2\text{T}_x@\text{GDY}$  at different voltages in the charging and discharging processes; CV curves at diverse sweeping rate of c)  $\text{Ti}_3\text{C}_2\text{T}_x$  and d)  $\text{Ti}_3\text{C}_2\text{T}_x@\text{GDY}$ , respectively. The capacitive contribution of e)  $\text{Ti}_3\text{C}_2\text{T}_x$  and f)  $\text{Ti}_3\text{C}_2\text{T}_x@\text{GDY}$  at  $1\text{ mV s}^{-1}$ , respectively.

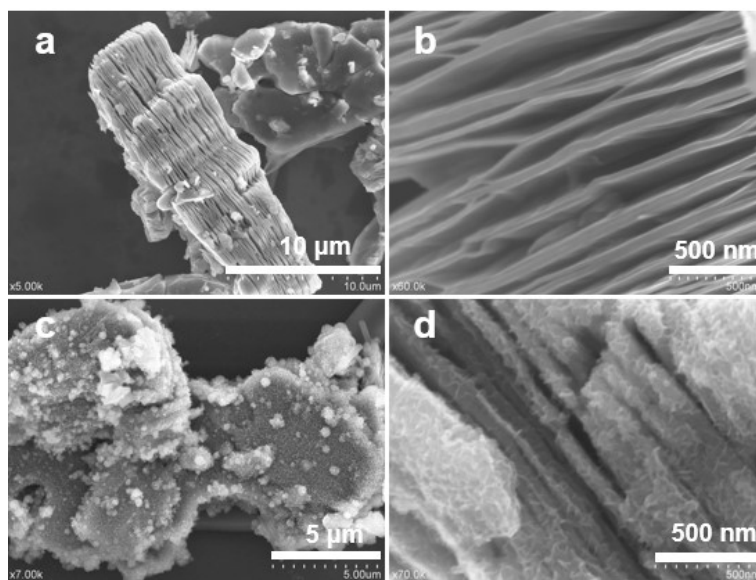


Figure S8. a) and b) the SEM images of the b- $\text{Ti}_3\text{C}_2\text{T}_x$ , c) and d) the SEM images of the b- $\text{Ti}_3\text{C}_2\text{T}_x@\text{GDY}$ .